Structural Features of Nanotubes Synthesized from NaOH Treatment on TiO_2 with Different Post-Treatments

Chien-Cheng Tsai and Hsisheng Teng*

Department of Chemical Engineering and Center for Micro/Nano Technology Research, National Cheng Kung University, Tainan 70101, Taiwan

Received August 17, 2005. Revised Manuscript Received September 25, 2005

We demonstrated that nanotubes synthesized from a NaOH treatment on TiO_2 with subsequent acid washing could proceed with repeatable crystalline-structure transformation through a simple acid−base washing step. By providing the unit cell parameters, we identified a divalent salt titanate ($Na_2Ti_2O_5 \cdot H_2O$) with a layered structure as the structure formed after the NaOH treatment. With the increase in acidity during the post-treatment acid washing, the layered titaniate transformed into a nanotube through Na^+-H^+ substitution, and eventually transformed into anatase TiO_2. Crystalline-structure analysis has shown the feasibility of this titanate−titania transformation occuring through a simple structural rearrangement. A complete scheme for the formation and transformation of nanotubes induced by the NaOH treatment and the post-treatment washing was proposed.

Introduction

Nanocrystalline metal-oxide semiconductors have been widely employed in photocatalytic or photoelectrochemical systems because of the large area of the solid-solution interface, where the interactions between the photon-induced charge carriers and the active species in the solution occur.[1,2] Among these semiconductors, TiO_2 has drawn much attention, and numerous efforts have been devoted to the synthesis of nanosized TiO_2.[3] Kasuga et al. reported that the thermal treatment of TiO_2 particles in NaOH resulted in the formation of anatase TiO_2 nanotubes with large surface areas.[4,5] Apart from the crystalline structure of anatase TiO_2,[4−12] some titanate structures, such as $A_2Ti_2O_5 \cdot H_2O$,[13,14] $A_2Ti_3O_7$,[15−23] $H_2Ti_4O_9 \cdot H_2O$,[24] and lepidocrocite titanates,[25,26] have been assigned as nanotube constituents (A = Na and/or H). Table 1 summarizes the nanotube structures proposed by different studies and the corresponding conditions for nanotube synthesis, which generally involved NaOH treatment followed by post-treatment washing. The treatment in NaOH (generally 10 N aqueous solution) was conducted either chemically (i.e., under atmospheric pressure) or hydrothermally (i.e., in a sealed autoclave) at 100−180 °C. The saturation pressure of 10 N NaOH aqueous solution at 100

* To whom correspondence should be addressed. E-mail: hteng@mail.ncku.edu.tw. Tel: 886-6-2385371. Fax: 886-6-2344496.

(1) (a) Hoffman, M. R.; Martin, S. T.; Choi, W.; Bahnemann, D. W. *Chem. Rev.* **1995**, *95*, 69. (b) Stone, V. F.; Davis, R. J. *Chem. Mater.* **1998**, *10*, 1468. (c) Ishikawa, Y.; Matsumoto, Y.; Nishida, Y.; Taniguchi, S.; Watanabe, J. *J. Am. Chem. Soc.* **2003**, *125*, 6558. (d) Zhao, W.; Ma, W.; Chen, C.; Zhao, J.; Shuai, Z. *J. Am. Chem. Soc.* **2004**, *126*, 4782. (e) Bao, N.; Shen, L.; Yanagisawa, K. *J. Phys. Chem. B* **2004**, *108*, 16739. (f) Peng, T.; Zhao, D.; Dai, K.; Shi, W.; Hirao, K. *J. Phys. Chem. B* **2005**, *109*, 4947. (g) Maeda, K.; Takata, T.; Hara, M.; Saito, N.; Inoue, Y.; Kobayashi, H.; Domen, K. *J. Am. Chem. Soc.* **2005**, *127*, 8286.
(2) (a) O'Regan, B.; Lenzmann, F.; Muis, R.; Wienke, J. *Chem. Mater.* **2002**, *14*, 5023. (b) Unal, U.; Matsumoto, Y.; Tanaka, N.; Kimura, Y.; Tamoto, N. *J. Phys. Chem. B* **2003**, *107*, 12680. (c) Park, H.; Choi, W. *J. Phys. Chem. B* **2004**, *108*, 4086. (d) Sakai, N.; Ebina, Y.; Takada, K.; Sasaki, T. *J. Am. Chem. Soc.* **2004**, *126*, 5851. (e) Yin, J.; Zou, Z.; Ye, J. *J. Phys. Chem. B* **2004**, *108*, 12790.
(3) (a) Miao, Z.; Xu, D.; Ouyang, J.; Guo, G.; Zhao, X.; Tang, Y. *Nano Lett.* **2002**, *2*, 717. (b) Cozzoli, P. D.; Kornowski, A.; Weller, H. *J. Am. Chem. Soc.* **2003**, *125*, 14539. (c) Jun, Y.-W.; Casula, M. F.; Sim, J.-H.; Kim, S. Y.; Cheon, J.; Alivisatos, A. P. *J. Am. Chem. Soc.* **2003**, *125*, 15981. (d) Zhu, H.; Gao, X.; Lan, Y.; Song, D.; Xi, Y.; Zhao, J. *J. Am. Chem. Soc.* **2004**, *126*, 8380. (e) Zhu, H. Y.; Lan, Y.; Gao, X. P.; Ringer, S. P.; Zheng, Z. F.; Song, D. Y.; Zhao, J. C. *J. Am. Chem. Soc.* **2005**, *127*, 6730.
(4) Kasuga, T.; Hiramatsu, M.; Hoson, A.; Sekino, T.; Niihara, K. *Langmuir* **1998**, *14*, 3160.
(5) Kasuga, T.; Hiramatsu, M.; Hoson, A.; Sekino, T.; Niihara, K. *Adv. Mater.* **1999**, *11*, 1307.
(6) Seo, D. S.; Lee, J. K.; Kim, H. *J. Cryst. Growth* **2001**, *229*, 428.
(7) Zhu, Y.; Li, H.; Koltypin, Y.; Hacohen, Y. R.; Gedanken, A. *Chem. Commun.* **2001**, 2616.
(8) Zhang, Q.; Gao, L.; Sun, J.; Zheng, S. *Chem. Lett.* **2002**, 226.
(9) Wang, Y. Q.; Hu, G. Q.; Duan, X. F.; Sun, H. L.; Xue, Q. K. *Chem. Phys. Lett.* **2002**, *365*, 427.
(10) Yao, B. D.; Chan, Y. F.; Zhang, X. Y.; Zhang, W. F.; Yan, Z. T.; Wang, N. *Appl. Phys. Lett.* **2003**, *82*, 281.
(11) Tsai, C. C.; Teng, H. *Chem. Mater.* **2004**, *16*, 4352.
(12) Wang, W.; Varghese, O. K.; Paulose, M.; Grimes, C. A. *J. Mater. Res.* **2004**, *19*, 417.
(13) Yang, J.; Jin, Z.; Wang, X.; Li, W.; Zhang, J.; Zhang, S.; Guo, X.; Zhang, Z. *J. Chem. Soc., Dalton Tans.* **2003**, 3898.
(14) Zhang, M.; Jin, Z.; Zhang, J.; Guo, X.; Yang, J.; Li, W.; Wang, X.; Zhang, Z. *J. Mol. Catal. A: Chem.* **2004**, *217*, 203.
(15) Du, G. H.; Chen, Q.; Che, R. C.; Yuan, Z. Y.; Peng, L. M. *Appl. Phys. Lett.* **2001**, *79*, 3702.
(16) Chen, Q.; Du, G. H.; Zhang, S.; Peng, L. M. *Acta Crystallogr., Sect. B* **2002**, *58*, 587.
(17) Chen, Q.; Zhou, W. Z.; Du, G. H.; Peng, L. M. *Adv. Mater.* **2002**, *14*, 1208.
(18) Tian, Z. R.; Voigt, J. A.; Liu, J.; Mckenzie, B.; Xu, H. *J. Am. Chem. Soc.* **2003**, *125*, 12384.
(19) Zhang, S.; Peng, L.-M.; Chen, Q.; Du, G. H.; Dawson, G.; Zhou, W. Z. *Phys. Rev. Lett.* **2003**, *91*, 256103.
(20) Sun, X.; Li, Y. *Chem.−Eur. J.* **2003**, *9*, 2229.
(21) Yuan, Z.-Y.; Su, B.-L. *Colloids Surf., A* **2004**, *241*, 173.
(22) Thorne, A.; Kruth, A.; Tunstall, D.; Irvine, J. T. S.; Zhou, W. *J. Phys. Chem. B* **2005**, *109*, 5439.
(23) Zhang, S.; Chen, Q.; Peng, L.-M. *Phys. Rev. B* **2005**, *71*, 014104.
(24) Nakahira, A.; Kato, W.; Tamai, M.; Isshiki, T.; Nishio, K. *J. Mater. Sci.* **2004**, *39*, 4239.
(25) Ma, R.; Bando, Y.; Sasaki, T. *Chem. Phys. Lett.* **2003**, *380*, 577.
(26) Ma, R.; Fukuda, K.; Sasaki, T.; Osada, M.; Bando, Y. *J. Phys. Chem. B* **2005**, *109*, 6210.

10.1021/cm0518527 CCC: $33.50
Published on Web 12/10/2005

Table 1. Nanotubes of Different Structures Prepared from Different TiO_2 Precursors, NaOH Treatment Conditions,[a] and Post-Treatment Washing Processes (in sequence)

precursor	NaOH treatment[a]	post-treatment	refs
Nanotube Structure: Anatase TiO_2			
anatase	hydro/110/20	HCl + water	Kasuga et al.[4]
rutile	chem/110/20	HCl + water	Kasuga et al.[5]
anatase	chem/150/12	water	Seo et al.[6]
anatase	hydro/110/20	HNO_3 + water	Zhang et al.[8]
anatase	chem/110/20	HCl + water	Wang et al.[9]
anatase	hydro/150/12	HNO_3 + water	Yao et al.[10]
anatase/rutile	hydro/130/24	HCl	Tsai and Teng[11]
anatase	chem/180/30	HCl + water	Wang et al.[12]
Nanotube Structure: Anatase TiO_2/$H_2Ti_3O_7$·$0.5H_2O$			
rutile	chemi/110/4[b]	HNO_3 + water	Zhu et al.[7]
Nanotube Structure: $A_2Ti_2O_5$·H_2O			
TiO_2 powder	chem/110/20	HCl + water	Yang et al.[13]
anatase	chem/110/20	HCl + water	Zhang et al.[14]
Nanotube Structure: $A_2Ti_3O_7$			
anatase	hydro/130/72	HCl + water	Du et al.[15]
anatase	hydro/130/72	HCl + water	Chen et al.[16]
anatase	hydro/130/72	water	Chen et al.[17]
anatase/rutile	hydro/150/20	water	Tian et al.[18]
any crystals	hydro/130/72	water	Zhang et al.[19]
anatase	hydro/180/48	water	Sun and Li[20]
anatase	hydro/180/24	HCl + water	Yuan and Su[21]
rutile	hydro/150/72	HCl + water	Thorne et al.[22]
anatase/rutile	hydro/130/72	water	Zhang et al.[23]
Nanotube Structure: $H_2Ti_4O_9$·H_2O			
anatase/rutile	hydro/110/96	HCl + water	Nakahira et al.[24]
Nanotube Structure: Lepidocrocite Titanates			
anatase	hydro/150/48	water + HCl	Ma et al.[25]
anatase	hydro/130/24	water + HCl	Ma et al.[26]

[a] Treatment conditions refer to chemical or hydrothermal processes, temperature (°C), and duration (h), respectively. [b] Sonication at 280 W before chemical treatment.

°C is 0.6 bar, and it increases to 1.2 bar at 120 °C and 4.1 bar at 160 °C.[27] The data suggest that the influence of the pressure difference on the products would not be significant for treatments conducted at temperatures lower than 150 °C. It has been reported that nanotubes have formed during the treatment in NaOH.[13,15−17] However, some other studies showed that intermediate phases were produced from the NaOH treatment, and that the post-treatment was a critical step for nanotube formation.[4,5,11,20] The influence of the post-treatment will be a focus in the present work.

Our previous study showed that high-porosity nanotubes (ca. 400 m^2/g in BET area) can be obtained from an acidic post-treatment washing at pH values of 1−2.[11] The high-porosity nanotube aggregates had an X-ray diffraction (XRD) pattern analogous to that of anatase TiO_2, rather than that of the titanates. Upon calcination of the nanotubes obtained from the acidic post-treatment, the samples showed a well-defined anatase phase in their XRD pattern, and also a rutile phase at higher temperatures, reflecting the absence of Na in the anatase nanotubes.[11] On the other hand, aggregates with lower porosities were obtained from washing at higher pH values.[11] The structure of these higher-pH aggregates will be shown later in the present work to be that of a titanate. Other previous studies claiming titanate structures for nanotubes generally reported a smaller surface area (less than 200 m^2/g).[17,24] It is thus anticipated that the acidity in the post-treatment washing plays a key role in determining the structure of the nanotubes.

The crystalline structures of anatase TiO_2 and titanates can be easily distinguished by their characteristic *d* spacing lengths. However, the characteristic *d* spacing lengths of the foregoing titanates proposed for the nanotubes are considerably similar.[13−26] Thus, the exact titanate structure that comprises the titanate nanotubes is still a controversial topic that is under debate.[13,16,24,25] The present work intends to not only shed light on the role of the post-treatment acidity but also give suggestions for the conflicting nanotube structures proposed in contemporary literature.

Experimental Section

The TiO_2 precursor used for nanotube production was a commercially available TiO_2 powder (P25, Degussa AG) that consisted of ca. 30% rutile and 70% anatase in crystalline phase. The preparation was initiated by treating 2 g of the P25 powder with 70 mL of 10 N NaOH in a Teflon-lined autoclave at 130 °C for 24 h. The process was analogous to those reported,[4,5] except that the present treatment was conducted hydrothermally rather than under atmospheric pressure. After the treatment and subsequent cooling, we subjected the precipitate from filtration to pH-value regulation by mixing it with 1 L HCl solutions of different concentrations. The final products were obtained by filtration with subsequent drying at 100 °C for 3 h. To determine whether the crystalline structure would reversibly change with the equilibrated pH value, we backwashed the precipitate from washing at the lowest pH (ca. 0.38), in the same manner as that for the HCl washing, with 1 L NaOH solutions of different concentrations for reaching higher pH values.

The phase identification of the nanotube samples from different synthesis processes was conducted with powder X-ray diffraction (XRD) using a Rigaku RINT2000 diffractometer equipped with Cu Kα radiation. The data were collected for scattering angles (2θ) ranging from 5 to 70° with a step size of 0.01°. The microstructures were explored with a high-resolution transmission electron microscope (HRTEM; Hitachi FE-2000). The pore structure was characterized by N_2 adsorption at −196 °C using an adsorption apparatus (Micromeritics ASAP 2010). The surface area of the samples was determined from the Brunauer−Emmett−Teller (BET) equation. The structural models of anatase TiO_2 and titanates assigned to nanotubes or other particulates were constructed with the Ca.R.Ine version 3.1 crystallography program package.[28]

Results

It is generally recognized that during treatment with concentrated NaOH, some Ti−O bonds of the TiO_2 precursor are broken, leading to the formation of lamellar fragments that are the intermediate phase in the formation process of the nanotube material.[5,13,19] It was reported that the condition of the post-treatment washing affected the formation, crystalline structure, or even chemical composition of the final nanotube products.[5,11,20] However, some other studies claimed that nanotubes were formed during the NaOH treatment, and that the acidic post-treatment was not essential in nanotube synthesis.[13,15−17] This contradiction in the experimental

(27) Perry, R. H.; Chilton, C. H. *Perry's Chemical Engineers' Handbook*, 7th ed.; McGraw-Hill Book Co.: New York, 1997.

(28) *Ca.R.Ine crystallography program package*, version 3.1; Ca.R.Ine Crystallography: Senlis, France, 1998.

findings most likely resulted from the difference in the severity of the NaOH treatment, i.e., the difference in temperature and the duration employed.[19,22,23] A severe treatment, with a high temperature or long duration, might have induced nanotube formation during NaOH treatment.[19,22,23] Agitation might accelerate the formation of nanotubes as well, as a study found that the formation of nanotubes was completed after 20 h of NaOH treatment at 110 °C with agitation.[13] On the other hand, a mild treatment, i.e., with a low temperature and short duration, would produce specimens in intermediate states that would proceed with further transformation into tubes through soft-chemical reactions in the post-treatment steps.[5,11,20] Therefore, the difference in NaOH treatment severity should be one of the main causes for the conflicts observed in the previous structural studies.

In the present work, the products obtained from NaOH treatment at 130 °C for 24 h contained no tubular structures, and were found to be sensitive to the post-treatment washing. After the samples were washed with HCl, nanotubes became the dominant component of specimens with a washing pH of less than 8. The specimens obtained by HCl washing to different pH values were analyzed by XRD. The diffraction patterns are shown in the upper portion of Figure 1. In the pH-decreasing course with HCl washing, there are characteristic peaks positioned at $2\theta = 9.8$, 24, and 28° (indicated by the dash lines in Figure 1). These peaks have been assigned to the diffraction of titanates such as $A_2Ti_2O_5 \cdot H_2O$,[13,14] $A_2Ti_3O_7$,[15−23] and lepidocrocite titanates.[25,26] The appropriate crystalline structure responsible for these diffraction peaks will be discussed in detail later. With the decrease in pH, there appears to be a corresponding decrease in the intensity of the 28° peak relative to that of 24° peak. This has been ascribed to the decrease in the Na:H ratio of the titanates caused by the replacement of Na^+ with H^+ during acid washing.[13] To examine this, we calcined the samples obtained by washing at different pH values at 700 °C for 1 h, and then subjected them to XRD analysis. The XRD patterns (Figure 2) show that $Na_2Ti_6O_{13}$, which could be derived from dehydration of the titanates, was the only Na-containing species detected, and it was more abundant for specimens obtained at a higher pH. This supports the argument that Na^+ and H^+ in the titanate were exchangeable with pH variation. However, the evidence of the present work strongly suggests that the change in the peak intensity ratio should mainly be caused by the gradual transformation of the crystalline structure.

With the washing pH lowered to 1.6, the 24° peak shifts to 25°, accompanied by a marked weakening of the 9.8 and 28° peaks, especially the former. The peak at 25° (indicated by a solid line in Figure 1) should correspond to the (101) diffraction of anatase TiO_2. Calcination of this sample to 700 °C showed only the presence of anatase and rutile (Figure 2). The specimen obtained by washing at this pH (1.6) should be composed of anatase (the major one) and protonic titanate. If the pH is further lowered to 0.38, the anatase TiO_2 appears to be the exclusive phase shown in the XRD pattern. The preceding results obtained with a progressive pH decrease have demonstrated a phase-transition

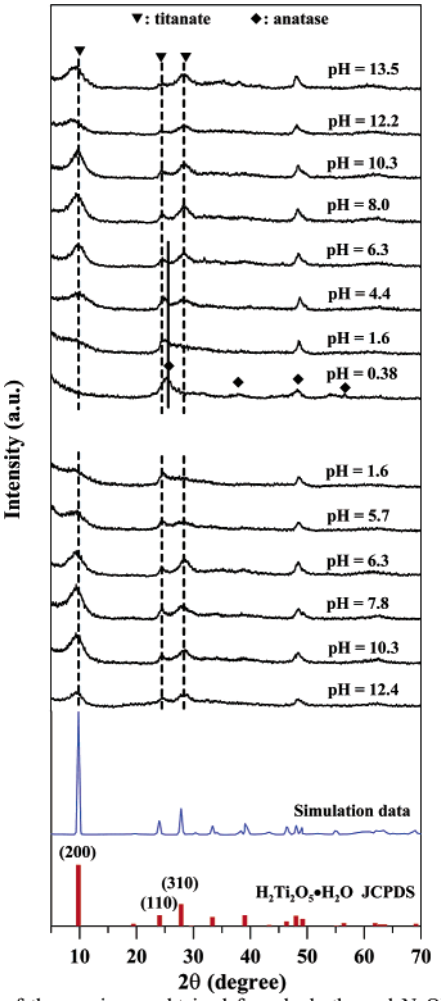

Figure 1. XRD patterns of the specimens obtained from hydrothermal NaOH treatment on TiO_2 at 130 °C with subsequent post-treatment washing at different pH values (the upper part). The middle part of the figure shows the patterns of the specimens by backwashing the pH = 0.38 sample (in the upper part) to different pH values. The standard diffraction pattern of $H_2Ti_2O_5 \cdot H_2O$ from JCPDS and the simulation data using the cell parameters shown in Table 2 are provided at the bottom of this figure.

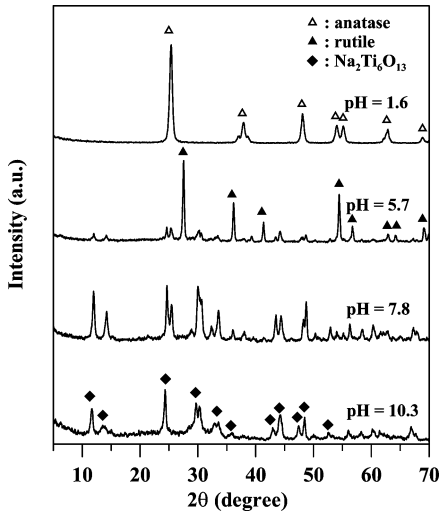

Figure 2. pH value dependence of the XRD pattern of the specimens obtained by calcining nanotube aggregates of different pH values at 700 °C for 1 h. The nanotube aggregates were prepared from a NaOH treatment on TiO_2 followed by washing with HCl to different pH values.

sequence of Na-containing titanate, protonic titanate, and finally anatase TiO_2. Instead of distinct phase transition, there

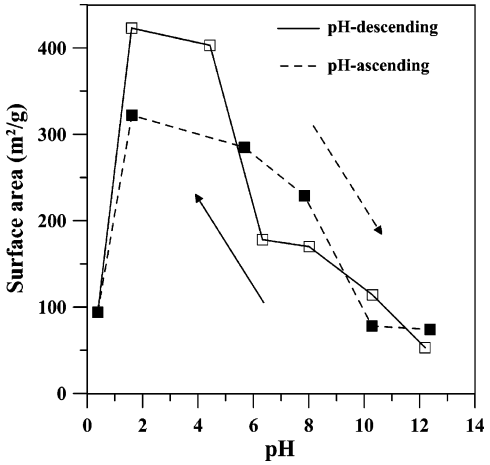

Figure 3. Surface area of the specimens obtained from post-treatment washing at different pH values. The pH-descending sequence was conducted by washing the NaOH-treated materials with HCl solutions of different concentrations. Following the acid washing, the pH-ascending sequence was conducted by washing the HCl-washed (pH = 0.38) specimen with NaOH solutions of different concentrations.

was a coexistence of neighboring phases in some pH regimes. Previous studies have reported the transformation of protonic titanate to anatase under acidic conditions.[3d,e]

By backwashing the pH = 0.38 sample with NaOH, we observed recovery of the titanate peaks (2θ = 9.8, 24, and 28°) in the XRD patterns, as shown in the middle portion of Figure 1, accompanied by weakening of the anatase (101) diffraction at 25°. The crystalline structure seems to change reversibly with the pH variation.

In addition to the crystalline structure, the morphology of the nanotubes, which can be to a certain extent indexed by the pore structure, was subjected to analysis using N_2 adsorption. The variation of the surface area with washing pH is depicted in Figure 3. In the pH-descending course, the area increases to reach a maximum at pH = 1.6, and it then decreases. At pH = 1.6, the nanotube aggregates should be in a loose configuration, because the porosity was contributed to by the internal space as well as the interstice of the nanotubes. The hysteresis loop of the N_2 adsorption−desorption isotherms supports this argument (see the Supporting Information). In the pH-ascending course starting from pH = 0.38, Figure 3 shows that the surface area increases to a maximum, also at a pH near 1.6, and then decreases, but the variation locus did not exactly follow that of the pH-descending course. The maximum area of the specimens in the pH-ascending course is smaller than that in the descending one. This suggests that the nanotube morphology formed from backwashing the anatase TiO_2 (obtained at pH = 0.38) is different from that formed by scrolling the titanate sheets with acid washing.[13,19] The variation in the XRD pattern and surface area of the nanotubes with the post-treatment pH shows that the microscopic crystalline structure is likely to be a thermodynamic product, whereas the macroscopic morphology is essentially path-dependent.

The TEM images of the samples obtained in the pH-descending course with acid washing are shown in Figure 4. The pH = 12.2 sample shown in Figure 4a contains granules composed of layered structure with an interlayer

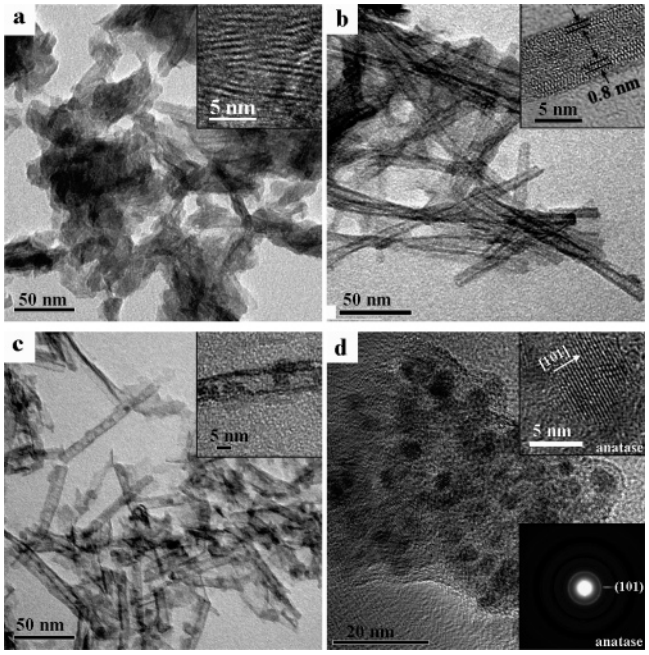

Figure 4. TEM images of specimens prepared from hydrothermal NaOH treatment on TiO_2 at 130 °C followed by washing with HCl to pH values of (a) 12.2, (b) 6.3, (c) 1.6, and (d) 0.38.

distance of ca. 0.8 nm, which is close to the reported interlayer distance of the nanotubes.[13,16,20] The layers would peel off with further acid washing, forming nanotubes.[13,19] Panels b and c of Figure 4 show the nanotubes obtained at pH values of 6.3 and 1.6, respectively. Nanotubes with intact walls can be observed for the pH = 6.3 sample, whereas there are defects on the walls of the pH = 1.6 sample.[15] The defects may be caused by the partial transformation of the titanate structure to anatase TiO_2 at this pH. With a further decrease in pH to 0.38, the structure transformed to coagulated particles, as shown in the TEM image in Figure 4d. The morphology explains the low porosity of the sample. However, only the lattice fringe of the anatase (101) faces can be observed from the TEM images (the upper inset), and only the (101) ring can be clearly seen in the selected area diffraction (SAED) pattern (the lower inset). This shows that the anatase TiO_2 formed under such a highly acidic environment comprises turbostratic stacking of the (101) faces with a defective alignment.

The TEM images of the specimens obtained by backwashing the pH = 0.38 TiO_2 with NaOH are shown in Figure 5. Figure 5a shows the appearance of nanotubes with an increase in pH to 1.6, though the tube shape cannot be well defined. In the formation of titanate nanotubes, it is obvious that hydration of anatase TiO_2 through a soft-chemical interaction with NaOH is less feasible than the route through scrolling the titanate sheets. This is also consistent with the observation obtained from the porosity variation, showing that the morphology was path-dependent. Further increasing the pH to 10.3 by backwashing shows the formation of plates (Figure 5b), for which the structure is found to be crystalline on the basis of the SAED pattern shown in the inset. This indicates that hydration of the pH = 0.38 anatase TiO_2 under a highly basic condition results in the formation of titanate (indicated by the XRD pattern) with a long-range crystalline order. Auxiliary experiments have shown that nanotubes can

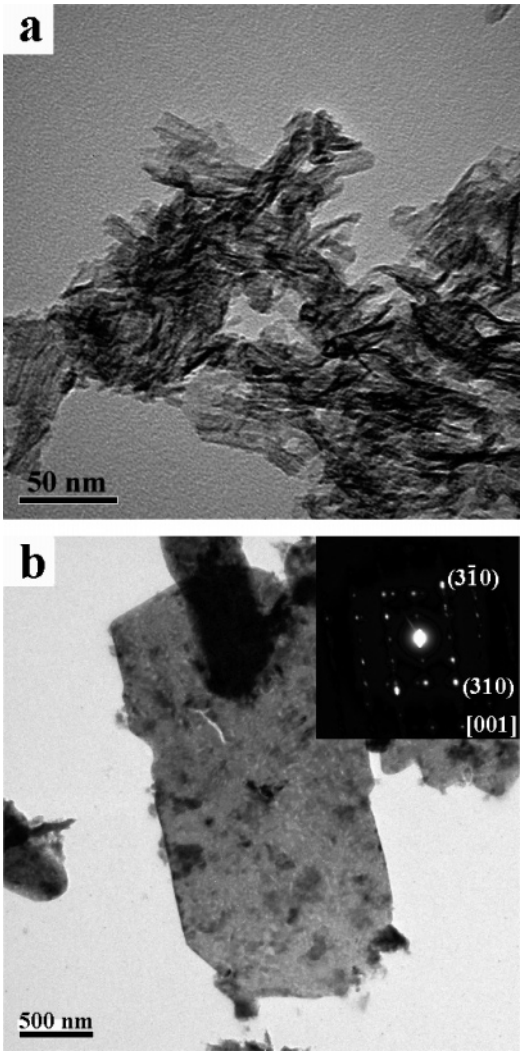

Figure 5. TEM images of specimens prepared by backwashing the HCl-washed (pH = 0.38) specimen with NaOH to pH values of (a) 1.6 and (b) 10.3.

be obtained by washing these plates with HCl. This nanotube formation should follow the peeling-off and scrolling mechanisms mentioned above.[13,19]

Discussion

Numerous studies on titanate nanotubes have reported XRD patterns similar to those of the titanate shown in Figure 1.[13−26] Peng and co-workers[16,17,19,23] have assigned protonic trititanate ($H_2Ti_3O_7$; monoclinic unit cell with $a = 1.603$ nm, $b = 0.375$ nm, $c = 0.919$ nm, and $\beta = 101.45°$) to be the building block of the nanotubes, which were seen forming during the treatment in NaOH. Theoretical studies have given the evolution mechanism as well as the stability of this $H_2Ti_3O_7$-type tubular structure in a concentrated NaOH environment.[19,23] On the other hand, one study[13] claimed that the nanotube material should be a divalent salt, $(Ti_2O_4(OH)_2)^{2-}$, on the basis of the reported XRD patterns of layered $H_2Ti_2O_5 \cdot H_2O$[29,30] and the dependence of Na^+-H^+ exchange on the pH value during the post-treatment washing. They suggested $Na_2Ti_2O_4(OH)_2$ (orthorhombic unit cell with $a = 1.926$ nm, $b = 0.378$ nm, and $c = 0.300$ nm) to be the structure obtained from the NaOH treatment and $Na_{2-x}H_xTi_2O_4(OH)_2$ after the post-treatment acid washing. Another study queried the validity of the trititanate nanotube model by pointing out a lack of prominent appearance of the trititanate (200) peak ($d = 0.786$ nm) in the XRD patterns of the nanotubes. They proposed a lepidocrocite-type titanate ($H_xTi_{2-x/4}\square_{x/4}O_4 \cdot H_2O$, with $\square$ = vacancy; orthorhombic unit cell with $a = 0.3783$ nm, $b = 1.8735$ nm, and $c = 0.2978$ nm) to coincide with the reflection peaks observed in the XRD patterns of the nanotubes.[25]

Both of the nanotube crystalline structures proposed against the trititanate, i.e., $Na_2Ti_2O_4(OH)_2$ and $H_xTi_{2-x/4}\square_{x/4}O_4 \cdot H_2O$, have been modeled to comprise lamellar sheets of edge-sharing TiO_6 octahedra.[13,25,30] Titanates of this layered structure could be readily exfoliated into monolayer nanosheets through a soft-chemistry route.[25] The XRD patterns of $H_2Ti_2O_5 \cdot H_2O$, which is identical to the protonic salt $H_2Ti_2O_4(OH)_2$, documented in the Powder Diffraction Files of the JCPDS[29] are shown at the bottom of Figure 1. The patterns of the titanate materials obtained in the present work are seen as being similar to those of $H_2Ti_2O_5 \cdot H_2O$. Thus, all the evidence suggests the nanotube structure should be assigned to layered $A_2Ti_2O_5 \cdot H_2O$. Although the layered structure has been indexed by the body-centered orthorhombic lattice projected normal along its sheet,[25,30] the positions of the interlayer ions (H^+, Na^+, and OH^-) were never reported. To obtain the complete atomic coordinates of this titanate, we have proposed, by incorporating the divalent salt and layered structural features,[13,25] a model for the $A_2Ti_2O_5 \cdot H_2O$ unit cell.

This modeling was conducted in an attempt to give the proximate coordinates of the interlayer atoms and thus the explanations for the observed nanotube formation and transformation. To avoid the complexity introduced by the Na^+-H^+ exchange, we considered the protonic structure as the major object in thr simulation at first. The lattice constants of the flat layered $H_2Ti_2O_5 \cdot H_2O$ employed were $a = 1.808$ nm, $b = 0.3797$ nm, and $c = 0.2998$ nm, and were obtained by referring to the file in the JCPDS.[29] The large elongation along the a axis was ascribed to the layered structure of the material.[30] By assuming the *Immm* space-group geometry that has been suggested for the lepidocrocite-type $H_xTi_{2-x/4}\square_{x/4}O_4 \cdot H_2O$,[31] we were able to visualize the unit-cell structure, shown in Figure 6. There are H_2O molecules, composed of exchangeable H^+ and OH^- ions, situated between the host layers of the body-centered lattice. In the two-dimensional sheets, TiO_6 octahedra are combined with each other via edge-sharing.[25] The positions of the H_2O molecules were determined by regression analysis to accord with the real XRD pattern. The bond distance of H^+-OH^- was assumed to be identical to that of H−O in H_2O, i.e., ca. 0.15 nm.[32] Table 2 lists the resulting atom positions of the

(29) *Powder Diffraction File of the Joint Committee on Powder Diffraction Standards*, Card 47-0124; International Centre for Diffraction Data: Newton Square, PA, 2002.
(30) Sugita, M.; Tsuji, M.; Abe, M. *Bull. Chem. Soc. Jpn.* **1990**, *63*, 1978.
(31) Sasaki, T.; Watanbe, M.; Hashizume, H.; Yamada, H.; Nakazawa, H. *J. Am. Chem. Soc.* **1996**, *118*, 8329.
(32) Tuckerman, M.; Lassonen, K.; Sprik, M.; Parrinello, M. *J. Chem. Phys.* **1995**, *103*, 150.

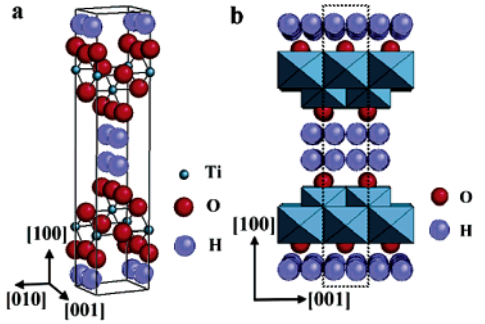

Figure 6. Proposed crystalline model for $H_2Ti_2O_5 \cdot H_2O$: (a) unit-cell structure of the basic cell of $H_2Ti_2O_5 \cdot H_2O$ and (b) representation of the refined crystal structure $H_2Ti_2O_5 \cdot H_2O$ projection along [010].

Table 2. Unit Cell Parameters (i.e., fractional coordinates) Used To Simulate the XRD Patterns of $H_2Ti_2O_5 \cdot H_2O$ Nanotubes Prepared from NaOH Treatment with Subsequent Acid Washing[a]

atom position	*x*	*y*	*z*	atom position	*x*	*y*	*z*
Ti(1)	0.2159	0	0	O(9)	0.7159	0	1/2
Ti(2)	0.2839	1/2	1/2	O(10)	0.7839	1/2	0
Ti(3)	0.7159	1/2	1/2	O(11)	0.8519	0	1/2
Ti(4)	0.7839	0	0	O(12)	0.8672	0	0
O(1)	0.1327	0	0	H(1)	1/20	0	1/4
O(2)	0.1479	0	1/2	H(2)	1/20	0	3/4
O(3)	0.2159	1/2	0	H(3)	9/20	1/2	1/4
O(4)	0.2839	0	1/2	H(4)	9/20	1/2	3/4
O(5)	0.3519	1/2	0	H(5)	11/20	1/2	1/4
O(6)	0.3560	1/2	1/2	H(6)	11/20	1/2	3/4
O(7)	0.6439	1/2	1/2	H(7)	19/20	0	1/4
O(8)	0.6479	1/2	0	H(8)	19/20	0	3/4

[a] All occupancies are equal to 1.0.

unit cell, in which the coordinates of the interlayer H_2O molecules are analogous to those of the lepidocrocite-type $H_xTi_{2-x/4}\square_{x/4}O_4 \cdot H_2O$.[31] The XRD pattern simulated using the foregoing lattice constants and the atom positions in Table 2 is shown at the bottom of Figure 1. The simulated pattern is in good agreement with those of the titanate nanotubes and the JCPDS data, especially for peaks other than the (200) peak.

The results of the present work and previous studies have shown that the H^+ in the interlayer H_2O is exchangeable with Na^+.[13,14,20] The structure of $Na_2Ti_2O_5 \cdot H_2O$ is modeled to be analogous to that of $H_2Ti_2O_5 \cdot H_2O$, preserving a body-centered orthorhombic lattice.[13] The bond distance of Na−O in NaOH is 0.23 nm,[33] which is larger than that of H−O in H_2O. Intercalation with Na^+ would result in a larger interlayer distance than that with H^+. This argument coincides with the data in Figure 1, showing a larger d_{200} (i.e., a smaller 2θ for the (200) reflection) for the Na-abundant specimens obtained at pH >12 (top of Figure 1). The lattice constants of the pH = 13.5 sample were determined from the XRD pattern (top of Figure 1) to be $a = 1.951$ nm, $b = 0.369$ nm, and $c = 0.289$ nm, similar to those values reported by studies claiming a structure of $Na_2Ti_2O_4(OH)_2$ for the nanotubes.[13,14] The lattice constants of $H_2Ti_2O_5 \cdot H_2O$ and $Na_2Ti_2O_5 \cdot H_2O$ suggested above would result in (200) XRD peaks situated at $2\theta = 9.8$ and 9.2°, respectively. The (200) peak position of the titanate nanotubes shown in Figure 1 also ranges between 9.2 and 9.8°. All the evidence clearly points out

(33) Rustad, J. R.; Felmy, A. R.; Rosso, K. M.; Bylaska, E. J. *Am. Mineral.* **2003**, *88*, 436.

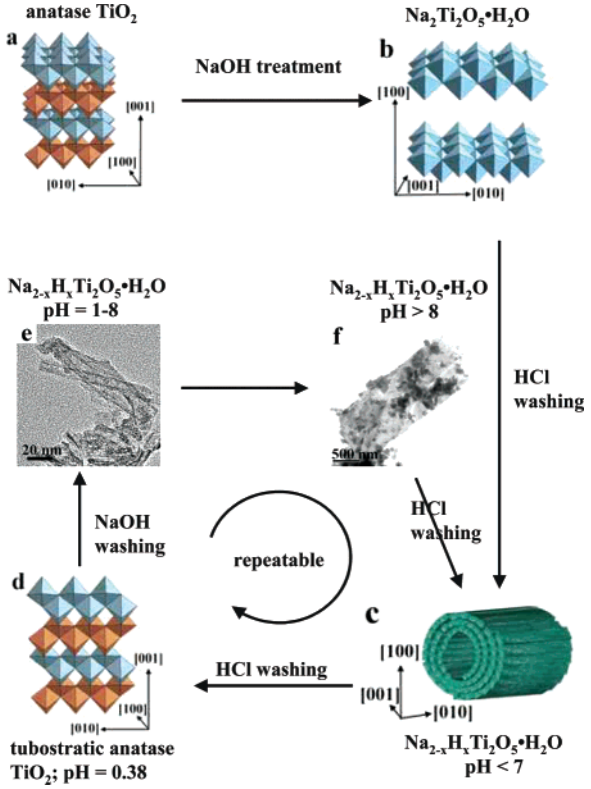

Figure 7. Overall scheme for the formation and transformation of nanotubes induced by the NaOH treatment and the post-treatment washing.

that $Na_{2-x}H_xTi_2O_5 \cdot H_2O$ is the structure of the titanate nanotubes, with the *x* value being a decreasing function of pH during post-treatment.

On the basis of the foregoing exploration, the formation and transformation of nanotubes induced by the NaOH treatment and post-treatment washing can be summarized in the scheme of Figure 7. Upon NaOH treatment, some of the Ti−O−Ti bonds are broken, forming an intermediate containing Ti−O−Na and Ti−OH. These intermediates would proceed with rearrangement to form sheets of edge-sharing TiO_6 octahedra with Na^+ and OH^- intercalated between the sheets. The formed structure is $Na_2Ti_2O_5 \cdot H_2O$ (i.e., $Na_2Ti_2O_4(OH)_2$). The projection along [001] of this sodium titanate exhibits layers of the TiO_6 octahedra edge-shared in a zigzag configuration (Figure 7b). This configuration can be correlated with the principal unit layer of the anatase TiO_2 projected along [101] (Figure 7a). A previous study also pointed out that if the two longer Ti−O bonds in the TiO_6 octahedra were broken, the anatase TiO_2 would transform into the layered titanate.[13] However, the literature summary in Table 1 has reflected that both anatase and rutile can be transformed into titanate nanotubes via the NaOH treatment. The rearrangement of the TiO_6 octahedra in rutile would thus be more vigorous in order to form the titanate. The exhibition of the anatase structure in Figure 7a simply intends to show the similarity between the principal structures of anatase and the titanate.

The formed $Na_2Ti_2O_5 \cdot H_2O$ would undergo Na^+ exchange with H^+ in the post-treatment acid washing. The exchange would result in variation of the surface charge, leading to a peeling-off of the individual layers of the titanate and subsequent scrolling of the layers into nanotubes (Figure

7c).[13,19] The *x* value of the nanotube structure, $Na_{2-x}H_xTi_2O_5 \cdot H_2O$, would increase with the acidity of the post-treatment. At an acidity as high as pH = 1.6, anatase becomes the major structure (Figure 1), rather than titanate. This indicates that the tube walls would proceed with dehydration,[3d] forming the anatase structure at some locations of the nanotubes. During this transformation, the titanate framework would shrink by reducing the interlayer distance. Because of the similar zigzag configuration, the [001] projection of the titanate layers would shrink to the (101) faces of anatase TiO_2, leading to a defective structure in the nanotubes. With a gradual increase in this transformation by increasing the post-treatment acidity, the nanotubes would eventually rupture to form small anatase crystallites, as depicted in the TEM image of Figure 4d. As stated above, the anatase thus derived was composed of turbostratic stacking of the (101) faces with a defective alignment (Figure 7d). Because of this defective feature, this anatase can be hydrated with intercalation, and can then transform into titanate nanotubes (Figure 7e) via a soft-chemical route, i.e., by backwashing with NaOH. When we further increased the pH in the backwashing to above 8, crystalline titanate plates would form (Figure 7f). When we washed the plates with HCl, nanotubes formed again (Figure 7c), most likely derived from scrolling of the titanate sheets. It appeared that, through stages c−f, the structure as well as the morphology of the specimens could be repeatedly cycled by varying the pH.

Knowledge of the transformation between titanate and TiO_2 would promote the application of this tubular-structure material. Because of the specific tubular feature, it has been shown that hydrothermal treatment of the nanotube suspensions under an acidic environment resulted in the formation of single-crystalline anatase nanoparticles with a specific crystal-growth direction (see the Supporting Information). By intercalating metal ions in the interlayer space of the tube wall and subsequently calcining the composite, we could obtain a high-activity catalyst, metal ion-planted anatase TiO_2, because of the highly dispersed active species (see the Supporting Information). The effectiveness of these applications would rely heavily on an appropriate tuning of the crystalline phase or texture feature of the nanotubes.

Conclusions

Upon hydrothermal treatment of TiO_2 in NaOH, a disordered phase with a layered structure formed in the present work. This disordered phase, believed to be the intermediate for nanotube formation, was mainly composed of $Na_2Ti_2O_5 \cdot H_2O$, a divalent salt titanate with an orthorhombic unit cell. After being washed with HCl, the disorder phase transformed into titanate nanotubes with the gradual substitution of Na^+ with H^+. When we increased the acidity of the washing, the nanotubes became defective because of the formation of an anatase TiO_2 phase on some spots of the tubes; they eventually transformed into nanocrystalline anatase with turbostratic stacking. By backwashing the nanocrystalline anatase with NaOH, we transformed the structure into titanate nanotubes and eventually to titanate plates at high pH values. Crystalline-structure analysis has demonstrated the possibility of the transformation between titanate and anatase TiO_2 being achieved through such a soft-chemical reaction route. Knowledge of this transformation could enormously extend the application of this specifically featured (large surface area and layered configuration) material.

Acknowledgment. This research is supported by the National Science Council of Taiwan (NSC 92-2214-E-006-021), the Center for Micro/Nano Technology Research at National Cheng Kung University, through projects from the Ministry of Education and the National Science Council (NSC 93-212-M-006-006) of Taiwan, and NCU-ITRI Joint Research Project of National Central University (NCU-ITRI 930202).

Supporting Information Available: N_2 adsorption−desorption isotherms for nanotube aggregates obtained with washing under different pH values; TEM image of TiO_2 nanorods obtained from hydrothermal treatment on a nanotube suspension; high activity of the Cu/nanotube catalyst in NO reduction with NH_3 (pdf). This material is available free of charge via the Internet at http://pubs.acs.org.

CM0518527